# Temperature effect on structural, mechanical properties and corrosion behaviour of CrN thin films deposited by magnetron sputtering

*Bassam Abdallah* ✉, *Mahmoud Kakhia, Walied Alssadat, Walaa Zetoun*

*Department of Physics, Atomic Energy Commission of Syria, P.O. Box 6091, Damascus, Syria*
✉ *E-mail: pscientific27@aec.org.sy*

Published in Micro & Nano Letters; Received on 10th October 2019; Revised on 5th May 2020; Accepted on 13th May 2020

Chromium nitride (CrN) thin films have been synthesised on Si(100) and stainless steel (SS304) substrates by direct current (DC) magnetron sputtering at different temperatures (25–100–200°C). The effects of temperature on structural and mechanical properties of the prepared films have been investigated. The CrN thin films have been described by X-ray diffraction to reveal their crystalline quality and texture. Results indicate that the grain size decreases with the temperature. The thickness of CrN films have been determined by scanning electron microscopy and their stoichiometry was measured by energy dispersive X-ray spectroscopy. Atomic force microscopy was employed to characterise the morphology of the surface for thin films and to calculate the roughness value. The results show that the hardness of films depends strongly on the grain size of the film. The micro-hardness of these films decreased with the increase in temperature. The corrosion of the CrN coating deposited was studied with corrosion potential, polarisation resistance, as well as electrochemical impedance spectroscopy techniques.

**1. Introduction:** Metal carbides and nitrides have been drawing much attention, as they are refractory compounds with high melting points, display resistance against corrosion, demonstrate electric and magnetic characteristics, which create potential substitutes for noble metals in various applications in material science [1, 2]. The transition metal carbides and nitrides have been oxidised in air and carbon dioxide by Clark [3], her results showed that the activation energies of the carbides were found to be lower than that found for the respective nitrides [3].

Transition metal nitride-based coatings such as titanium nitride (TiN) [4, 5], chromium nitride (CrN), tantalum nitride (TaN), zirconium nitride (ZrN), TiN/ZrN [6, 7], and niobium nitride (NbN) are used in coating industries due to their chemical, mechanical, tribological, and electrical properties. Choe *et al.* [8] reported that TiN coating of the implant surface prevents fracture due to fatigue under the physiological load surrounding the implant fixture. TiN nanocrystalline films deposited by magnetron sputtering in different bias voltages were studied by Chun [4]. Additionally, TiN films were deposited by reactive magnetron sputtering by Merie *et al.* [9], their results highlighted an important influence of temperature on the mechanical as well as tribological properties of TiN films. Vacuum arc discharge was used to obtain ZrNx films studied at different nitrogen ($N_2$) partial pressure ratios by Abdallah *et al.* [10], they established that residual stress and nitrogen incorporation in the film play an important role in the modification of micro-hardness [10].

CrN films possess high hardness, good wear, corrosion resistance, and good thermal stability, CrN thin films have been used in a variety of applications such as cutting tools, protective coatings in the food and medical industries, automotive industry, and microelectronics. In addition, they can be used in corrosive and high-temperature environments. Tribological and mechanical properties of CrN coatings grown on steel substrates using the magnetron sputtering technique were analysed by Ruden-Muñoz *et al.* [11], their films were developed at two pressures (0.4 and 4.0 Pa), good adherence behaviour was observed for films deposited at a low pressure [11]. The influence of both the partial nitrogen pressure and different gaseous percentage on their microstructural properties was investigated by Shah [12]. Liu *et al.* [13] found the hardness of CrN coating decrease with temperature, where the hardness of 2 mm thick CrN coating was varied between 21 and 10 GPa, during the increase of temperatures from 25°C to 500°C. Zalnezhad *et al.* [14] reported that CrN film has been identified as one of the most encouraging protective coatings on surfaces of tools and due to its excellent mechanical properties [14]. Bouzid *et al.* [15] have conducted a comparative study to evaluate the performances against wear and corrosion of CrN, CrMoN, CrZrN, CrVN single layer thin films. The CrN coating presented the better tribological properties than the ternary nitride coatings [15].

The surface films processing has a positive impact on adjustment and reinforcement of the surface functionality, e.g. surface procedures contain physical vapour deposition (PVD), chemical vapour deposition (CVD), thermal spraying, cladding, and electroplating [16]. CVD methods are not common, compared with PVD, because all precursors are solids and less efficient due to the difficulty in handling the gas flow. Additionally, high temperatures are required to induce this process [17].

CrN coating can be produced by various PVD methods such as hollow cathode deposition, plasma enhanced CVD [18], vacuum arc discharge and DC [19] or radio frequency magnetron sputtering [20]. In the magnetron sputtering method, the advantages are high deposition rate, good uniformity, and the low temperature of the substrate through the deposition. Subramanian and Jayachandran [19] have studied the corrosion performance of CrN films in 3.5% sodium chloride (NaCl) solution via electrochemical techniques. The process parameters in this technique are the substrate temperature, the sputtering pressure, the distance between the target and the substrate, substrate bias, target power, and deposition time [21]. Merie *et al.* [22] pointed out an important influence of the substrate temperature on teratology and mechanical properties of the CrN films [22].

In this work, CrN films have been grown by the DC magnetron sputtering method at different substrate temperatures. The materials of the substrate are (100) silicon and stainless steel (SS304). The energy dispersive X-ray spectroscopy (EDX) analysis method was employed to reveal information about the composition of the films. The structural properties of the films were described by X-ray diffraction (XRD). The thickness of these films has been determined by scanning electron microscopy (SEM). The mechanical properties (stress and microhardness) were characterised for deposited films. The corrosion was studied with electrochemical impedance spectroscopy (EIS) techniques. Results allow the




doi: 10.1049/mnl.2019.0600

determination of the influence of temperature on the structural and mechanical properties and corrosion behaviour of the deposited CrN films.

**2. Experimental procedure:** Magnetron sputtering with DC power, using a home manufacturing deposition system, has been used to produce CrN films at different temperatures. The films were deposited on silicon [Si(100)] and stainless steel (SS304) substrates. The chromium target's (purity 99.9%) diameter was 5 cm with a 5 cm distance. The vacuum in the deposition chamber was about $2 \times 10^{-6}$ Torr, the pressure and power were about 4 mTorr and 100 W, respectively. The thickness was measured using SEM (model TSCAN Vega II XMU) equipped with EDX. The structural properties of deposited films have been investigated by XRD with the $\theta$–$2\theta$ scan configuration (Stoe transmission X-ray diffractometer Stadi P). The morphology was acquired by SEM measurements, and the elementary composition and stoichiometry of the CrN films were defined by EDX. Measurements of microhardness were performed using Vickers indenter (load value 10 gf). The morphology of the films before and after the corrosion test was investigated by atomic force microscopy (AFM) [23] and optical microscopy.

A Voltalab PGZ 301 (France) test was carried out for corrosion (cell of 50 ml capacity) using the Tafel extrapolation method [24] and EIS techniques. The studies were carried out in sea water solution (3.5% NaCl) at 25°C with a scan rate of 1 mV/s and electrode potential (−1000 to +300 mV). In the EIS measurement, a sinusoidal AC perturbation of 10 mV was applied to the electrode at its corrosion potential ($E_{corr}$). The impedance data is collected within a frequency range of 100 kHz to 100 MHz, the rotation speed of the working electrode was 100 rpm.

**3. Results and discussion**

3.1. SEM and EDX analysis: The films deposited on Si(100) were characterised by SEM to reveal information about thickness, it was found that about 750 nm films were deposited at 25°C and 950 nm CrN deposited at 100°C as shown in Figs. 1*a* and *b*, which correspond to the deposition rate range between 21 and 27 nm/min, respectively. Shah *et al.* [25] found the decrease of the thickness with the increase of the temperature for pressure 10 mTorr. However, it increases the pressure of 20 mTorr. In our previous work [5] we found contrary behaviour for TiN film where the thickness increased with temperature from 50 to 300°C.

The compositions of the films were examined by EDX, Fig. 2*a* shows the EDX spectrum of the films for different temperatures and confirms the stoichiometry CrN of the film, where the observed presence of low contamination of oxygen (<5%). Fig. 2*b* shows the atomic percentage of CrN film at different temperatures. All samples were observed with a N/Cr ratio varied between 0.77 and 0.84, where oxygen contamination decreases and nitrogen content increases with increasing temperatures from 25 to 200°C. We can explain this phenomenon by degassing the residual air with an increase of the substrate temperature. These variations propose that the nitride component is successful at the expense of oxide components at higher temperatures. In [5], we found a similar behaviour with temperature for TiN film.

3.2. Structural characterisation (XRD): The spectra of the film deposited show two diffraction peaks at 37.60° and 43.70° assigned to (111) and (200) crystallographic planes in CrN/Si film, respectively (Fig. 3*a*), according to the JCPDS PDF no. 76-2494. The phases and preferred orientation of CrN thin films were measured by XRD. For each (*hkl*) plane, the grain size of films was calculated using the Scherrer formula [26]. The grain size of CrN thin films is calculated and plotted against substrate temperatures as shown in Fig. 3b. Whereas, the grain sizes of (111) and (200) peaks for CrN films deposited on Si (100) decrease with increase in temperatures. The higher grain size of the CrN coating at higher temperatures can be attributed due to better diffusivity of atoms assisting the grain growth. It is consistent with the published literature [27], but inconsistent with the literature [28]. The variations in the surface morphology of the CrN coatings occurred due to the mobility of grain boundaries. The effect of temperature on the XRD peak intensity of CrN thin films deposited on the Si substrate, while keeping the remaining parameters constant as shown in Fig. 3*c*. The films exhibit (111) preferred orientation and changes with temperature. It is found that the (200) orientation becomes a preferred orientation at 100°C. The texture coefficient [29, 30] of the CrN film as a function of temperature is calculated from the ratio of the *hkl* for a peak intensity of orientation relative to the average of the two orientations [23].

The texture coefficient is affected by the temperature during the deposition in our study (Fig. 3*c*). Other factors, besides the substrate effect, influence the film growth mechanism and its consequent quality (structure), such as deposition rate and residual gases (in particular oxygen), which can be incorporated into the film

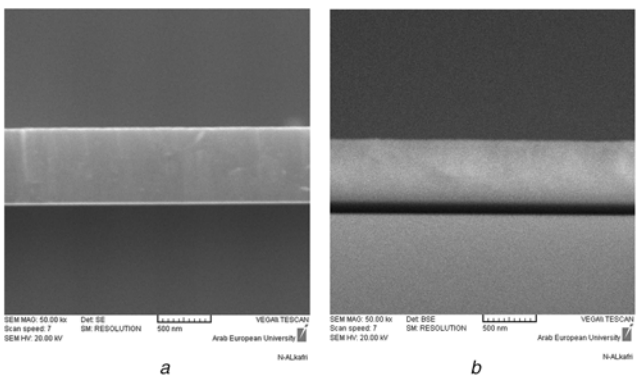


**Fig. 1** *SEM cross-section images for CrN/Si films prepared at*
*a* 25°C
*b* 200°C

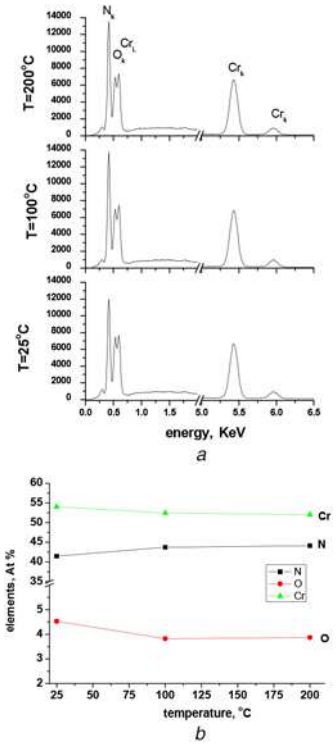


**Fig. 2** *Films deposited at different temperature*
*a* EDX spectrum of CrN/Si
*b* Elements percentage in CrN/Si film as a function of the temperature

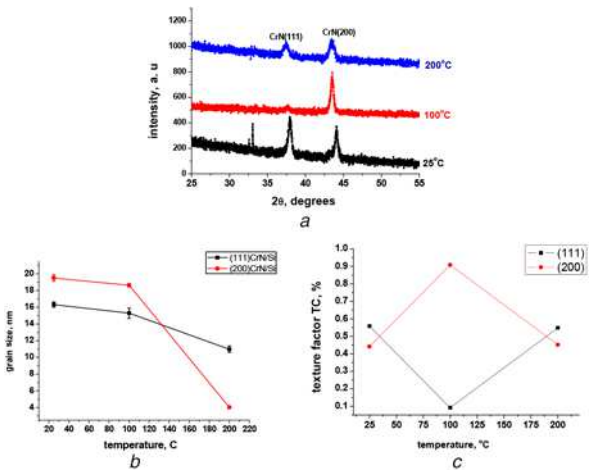


**Fig. 3** *Deposited at different temperature*
*a* XRD pattern of CrN/Si films
*b* Grain size as a function of the temperature
*c* Texture factor for deposited films as a function of the temperature

during deposition [10]. The substrate affects the grain size and crystalline quality, therefore different values of a deposited film on two different substrates; Si and SS304 were observed. In previous work, we also demonstrated the substrate influences on other films [31]. Additionally, the power and temperature affect the structure and therefore influence the crystallinity [5, 28].

3.3. Morphology study: The surface morphology study of the deposited films on Si substrates was observed by AFM. Fig. 4 illustrates two-dimensional AFM images of the CrN thin film at a scale of 2 × 2 µm. The observed surface of the deposited film was homogenous and smooth in both images of the deposited film at 25°C (Fig. 4*a*) and 200°C (Fig. 4*c*). However, the surface of the deposited film at 100°C (Fig. 4*b*) was rough due to the texture coefficient (TC) mentioned in Fig. 3*c*, where the dominant texture coefficient for (200) orientation was about 98%.

The roughness average (Ra) and root mean square (RMS) roughness are obtained from AFM measurements. We noticed that the

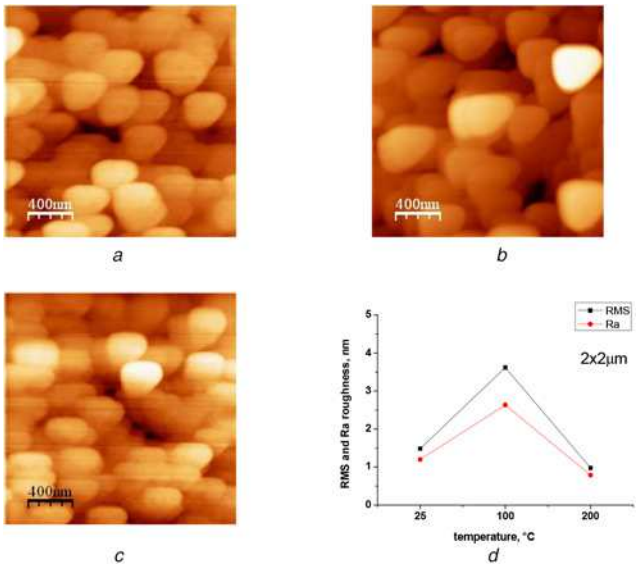


**Fig. 4** *AFM surface morphology 2D images at*
*a* 25°C for CrN/Si film
*b* 100°C for CrN/Si film
*c* 200°C for CrN/Si film
*d* RMS and Ra evolution as a function of temperature

RMS values were higher than those of Ra. They demonstrated values of 2.6 and 3.6 nm at 100°C, respectively. Small values were noticed for both films deposited at 25°C and 200°C as shown in Fig. 5*d*. This behaviour can be associated with the crystallinity of the films as shown in the XRD study above, where the (200) peak dominated at 100°C. In previous work, we observed a correlation between the roughness and the crystallographers [30]. The obtained values of roughness were less than those obtained by Shah *et al.* [25] for CrN film at different temperatures (200–400°C) due to the grain size of (111) orientation.

3.4. Strain measurement: The interplanar distance $d$ is obtained from the position of the (111) peak using Bragg condition from XRD patterns. Then the strain is calculated from $\varepsilon = (d - d_0)/d_0$ equation, where $d$ is the $d$-spacing from each film and $d_0$ is the $d$-spacing unstrained for CrN(111) orientation. It has been found that the strain is negative because $d < d_0$ (where $d_0 = 0.39654$ nm according to JCPDS no. 76-24964) and the peak is shifted to the right side, which indicates the existence of compressive stress in the studied films. Fig. 5 shows the variation of strain for the deposited films with temperature. It can also be seen that the compressive stress has almost similar behaviour with the grain size [28] as a function of temperature. The average stress deposited in CrN films is affected mainly by the plasma parameters [28]. Similarly, power density also affects the intrinsic stress of the CrN film by influencing the effect of other deposition parameters, it has been reported in the literature [27].

3.5. Microhardness measurement: Fig. 6 shows Vickers hardness of CrN/SS304 films deposited as a function of the temperature at 10 gf load, where the indentation was made on four different points in each CrN/SS sample to obtain its average hardness value. The value of microhardness decreased with increasing temperature from 26.3 to 16.1 GPa, this behavior agrees with grain size, which decreases with increasing temperature, associated with low roughness value. These values of micro hardness were greater

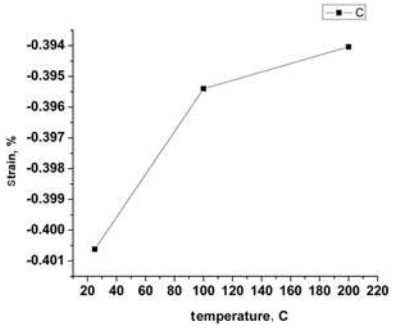


**Fig. 5** *Strain in CrN/Si films as a function of the temperature*

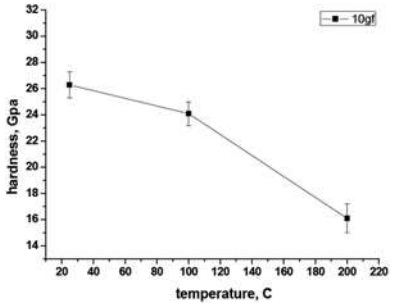


**Fig. 6** *Microhardness evaluation for films deposited on SS304 substrate as a function of the temperature*




doi: 10.1049/mnl.2019.0600

than the values obtained by Shah *et al.* [25] for CrN film, because the grain size of our films was smaller. Abdallah *et al.* [10] revealed and correlated the alteration of grain size and crystallographic texture with ZrN film. Several factors may contribute to the observed hardness behaviour of the metal nitride films, such as crystallographic texture (grain size), stoichiometry, and stress. Liu *et al.* [13] found the hardness of CrN coating decrease with temperature, the hardness of 2 mm thick CrN coating was varied between 21 and 10 GPa, where the temperature increased from 25 to 500°C. It is proven that the formed chromium oxide film was found to enhance the theological properties, while at higher temperatures the chromium oxide influenced lubricating function [32]. This was in accordance with the present study.

### 3.6. Corrosion measurements

3.6.1. Potential dynamic polarisation (Tafel): Fig. 7 shows the polarisation curve and its Tafel fit for the uncoated sample (SS304 substrate) and CrN/SS304 films deposited at different substrate temperatures. The electrochemical parameters in the Tafel method are characterised by Frankel [33], where the corrosion potential ($E_{corr}$) is presented in the *x*-axis, also the corrosion current density ($I_{corr}$) is presented in the *y*-axis. The corrosion parameters are usually proportional to the current density of corrosion [34]. The corrosion is tested in normal saline solution (3.5% NaCl at 25°C, which is equivalent seawater).

Table 1 summarizes the $E_{corr}$ and $I_{corr}$, where the smallest value (best corrosion resistance behaviour) of Icorr is 0.9827 μ A/cm$^2$ for the deposited CrN film by DC magnetron sputtering at 25°C, which is due to its smoothness and/or structure (grain size).

The present study shows that all CrN/SS304 films have lower corrosion rates (i.e. better corrosion resistance) than the SS304 substrate (uncoated) in the corrosive medium.

### 3.7. Electrochemical impedance spectroscopy (EIS)

To investigate the corrosion behaviour of PVD hard coating [30], it was well-known that EIS has found its efficacy. EIS is an interesting analytical method, because it can give a large quantity of information on corrosion reactions, such as mass transport. Over the frequency bandwidth of interest, the impedance is presented by the Nyquist plots [35]. EIS measurements were performed in a water solution after keeping them at autoclave steriliser. The Nyquist diagrams of the experimental results are shown in Fig. 8*a*. The experimental curves are fitted based on an equivalent circuit using the EC-Lab impedance programme, Fig. 8*b* shows the experimental and fitting plot for the film deposited at 25°C. A circuit model was proposed to describe two sub-electrochemical interfaces generally used in such cases [32]. The equivalent circuit for substrate (SS304) consists of $R_1$ and $Q_2$ corresponding to the solution resistance of the electrolyte test and constant phase element, respectively. $Q_1$ and $R_2$ elements are used in parallel to replace the coating dielectrics properties. $Q_3$ and $R_3$ in parallel are adapted to describe charge transfer at the coating/substrate interface. The impedance parameters, polarisation resistance $R_p$ ($=R_2+R_3$), and constant phase element $Q$ were calculated from Nyquist plots using the EC-lab programme.

$R_p$=4156 Ohm cm$^2$ for SS304 sample (uncoated) after the Nyquist fitting. All the impedance parameters of CrN films deposited on the SS304 substrate at different temperatures (25–200°C) are summarised in Table 2. It was noticed that the corrosion resistances for these films decrease from 53,260 to 10,747 Ohm cm$^2$ with increasing temperature from 25 to 200°C. In recent work, we found the corrosion resistance of these films decreases with increasing the current [24], however, the grain size increased due to the current effect. The film deposited at 25°C presents the best corrosion resistance and lower $Q_1$ value, while the film deposited at 200°C presents the lowest corrosion resistance because the film has the biggest grain size and the lowest hardness. Consequently,

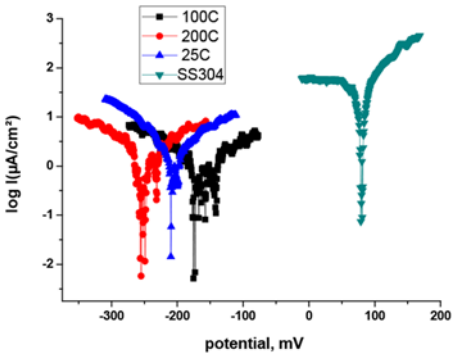


**Fig. 7** *Potential dynamic polarisation curves of SS304 substrate and CrN/SS304 films in 3.5% NaCl at 25°C*

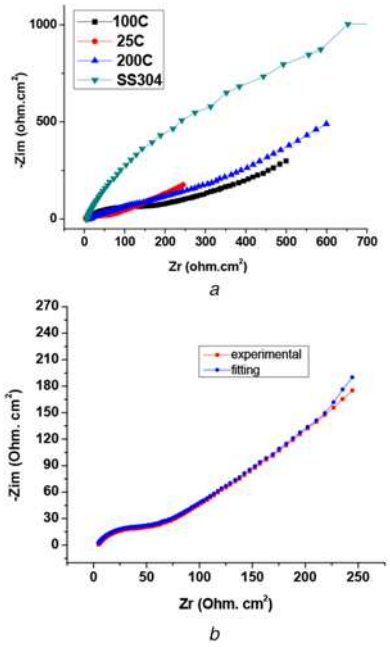


**Fig. 8** *EIS data*
*a* Nyquist plots of CrN films at different temperature (25–100–200°C)
*b* Fitting plot for film deposited at 25°C

**Table 1** Potential dynamic polarisation data by Tafel extrapolation method

| | $i_{corr}$, μA/cm$^2$ | $E_{corr}$, mv |
|---|---|---|
| 25°C | 0.9827 | −175.2 |
| 100°C | 1.5220 | −251.0 |
| 200°C | 3.6382 | −208.5 |
| reference SS304 | 31.678 | 79.9 |

**Table 2** Impedance parameter ($R_1$, $Q_1$, $a_1$, and $R_p$) for three films deposited on SS304 for different substrate temperature

| Temperature | $R_1$, Ohm cm$^2$ | $Q_1$, F s$^{(a-1)}$ | $a_1$ | $R_p$, Ohm cm$^2$ |
|---|---|---|---|---|
| 25°C | 7.684 | $61.62\times10^{-6}$ | 0.748 3 | 53,260 |
| 100°C | 12.73 | $3.112\times10^{-3}$ | 0.425 8 | 37,438 |
| 200°C | 4.542 | $0.115\ 3\times10^{-3}$ | 0.683 4 | 10,747 |

the EIS data indicate the existence of two different interfacial reactions which can be related to the film/solution interface and substrate/solution interface, respectively.

3.8. Morphology surface: The surface morphology before and after the corrosion experiment was investigated by using an optical microscope with magnifications 250× and 1200×, as shown in Figs. 9 and 10 for substrate and film deposited at 25°C, respectively. The lines appear as sharp edges due to the paper polishing of SS304 (Figs. 10*a* and *b*). Pitting corrosion is clearly shown as well as unsharp edges after the corrosion test in Figs. 10*c* and *d*.

Fig. 10 shows the optical microscopy surfaces of the deposited-film at 25°C (Figs. 10*a* and *b*) for CrN/SS304 before corrosion with magnification −250× and 1200×, respectively. Figs. 10*c* and *d* presents the surfaces of the film of CrN/SS304 after corrosion with magnification of 250× and 1200×, respectively. The film has few pitting corrosion after the corrosion measurements (Figs. 10*c* and *d*). These images confirmed the smooth morphology of the films as AFM study revealed. The corrosion behaviour of TiN coated stainless steel in an artificial physiological solution was investigated by Braic *et al.* [36], where the corrosion experiments showed that the corrosion behaviour of the coatings depends on the main deposition parameters, and the results were related to the influence of the deposition parameters on the chemical composition and morphology of the surface of the coatings.

The corrosion-electrochemical behaviour is normally related to the surface roughness, it is associated with a change of the dominant processes of the reduction oxidation reaction. Abdallah *et al.* [24] expressed a similar explanation and they have found that the Ti6Al4V/ SS304 films have improved better corrosion resistance than SS304 substrate in 0.9% NaCl at 37°C using potentiodynamic polarisation curves [24]. Generally, the surface of the deposited film has lower roughness (more smoothness) than uncoated samples approximately. Consequently, the CrN film resisted the aggressive action of the corrosion environment.

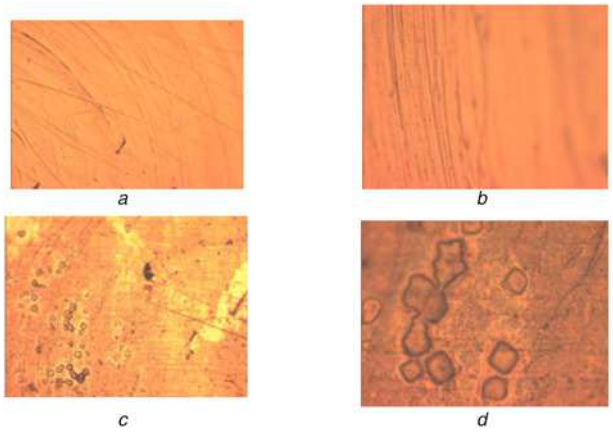


**Fig. 9** *Optical microscopy images of SS304*
*a* Before corrosion: magnification 250× for film
*b* Before corrosion: magnification 1200× for film
*c* After corrosion: magnification 250× for substrate tested in 3.5% NaCl
*d* After corrosion: magnification 1200× for substrate tested in 3.5% NaCl

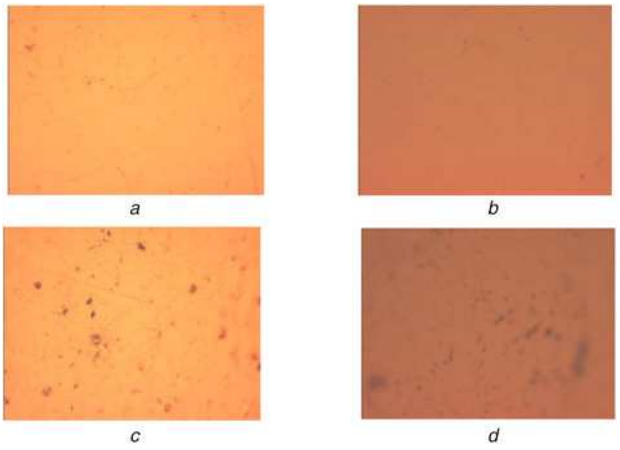


**Fig. 10** *Optical microscopy images of CrN/SS304*
*a* Before corrosion: magnification 250× for film
*b* Before corrosion: magnification 1200× for film
*c* After corrosion: magnification 250× for film deposited at 25°C in 3.5% NaCl
*d* After corrosion: magnification 1200× for film deposited at 25°C in 3.5% NaCl

**4. Conclusion:** CrN films have been successfully prepared by the DC magnetron sputtering technique at different temperatures (25–200°C). The composition of the films has been determined by the EDX technique; it has shown that the film approaches stoichiometric CrN. The grain size of (111) preferred orientation as well as the strain have been found to decrease with temperature. We have observed that the microhardness and grain size decreased with increasing temperature. A maximum hardness value of 26.3 GPa is obtained for CrN film deposited at 25°C. Residual stress and microhardness were found to be in agreement with the behavior of the corrosion of investigated the CrN/SS304 films by potential dynamic polarization and EIS techniques. The corrosion resistance for the films decreased with increasing temperature. The CrN film deposited at 25°C presents the best corrosion resistance and the highest hardness. The morphology of the films after and before the corrosion test was investigated by AFM and optical microscopy. The results indicate that the prepared films of CrN have better corrosion resistance compared with the SS304 substrate.

**5. Acknowledgments:** The authors acknowledge Professor I. Othman, the director of the atomic energy Commission of Syria and Dr S. Rihawy for fruitful discussions.

## 6 References

[1] Alhajri N.: 'Synthesis of IV–VI transition metal carbide and nitride nanoparticles using a reactive mesoporous template for electrochemical hydrogen evolution reaction'. Doctor of Philosophy, King Abdullah University, 2016
[2] Zeghni A.: 'The effect of thin film coatings and nitriding on the mechanical properties and wear resistance of tool steel'. Master's Eng., Dublin City University, 2003
[3] Clark J.: 'The reactivity of some transition metal nitrides and carbides'. Doctor of Philosophy, Plymouth University, 1995
[4] Chun S.-Y.: 'Bias voltage effect on the properties of tin films by reactive magnetron sputtering', *J. Korean Phys. Soc.*, 2010, **56**, (4), pp. 1134–1139
[5] Ismail I.M., Abdallah B., Abou-Kharroub M., *ET AL.*: 'XPS and RBS investigation of $TiN_xO_y$ films prepared by vacuum arc discharge', *Nucl. Instrum. Methods Phys. Res. B, Beam Interact. Mater. At.*, 2012, **271**, pp. 102–106
[6] Lin M.-T., Wan C.-H., Wu W.: 'Enhanced corrosion resistance of SS304 stainless steel and titanium coated with alternate layers of TiN and ZrN in a simulated $O_2$-rich environment of a unitized regenerative fuel cell', *Int. J. Electrochem. Sci.*, 2014, **9**, pp. 7832–7845
[7] Naddaf M., Abdallah B., Ahmad M., *ET AL.*: 'Influence of $N_2$ partial pressure on structural and microhardness properties of TiN/ZrN multilayers deposited by Ar/$N_2$ vacuum arc discharge', *Nucl. Instrum. Methods Phys. Res. B, Beam Interact. Mater. At.*, 2016, **381**, pp. 90–95
[8] Choe H.-C., Ko Y.-M., Park H.-O.: 'Electrochemical behavior of tin film coated Ti–Nb alloys for dental materials', *Met. Mater. Int.*, 2006, **12**, (4), pp. 365–369
[9] Merie V.V., Birleanu C., Pustan M.S., *ET AL.*: 'Analysis on temperature effect on the mechanical and tribological properties of titanium




doi: 10.1049/mnl.2019.0600

nitride thin films', *IOP Conf. Ser., Mater. Sci. Eng.*, 2016, **147**, p. 012019
[10] Abdallah B., Naddaf M., A-Kharroub M.: 'Structural, mechanical, electrical and wetting properties of ZrNx films deposited by $Ar/N_2$ vacuum arc discharge: effect of nitrogen partial pressure', *Nucl. Instrum. Methods Phys. Res. B, Beam Interact. Mater. At.*, 2013, **298**, pp. 55–60
[11] Ruden-Muñoz A., Restrepo-Parra E., Sequeda F.: 'Crn coatings deposited by magnetron sputtering: mechanical and tribological properties', *Dyna*, 2015, **82**, (191), pp. 147–155
[12] Shah H.N.: 'Structural and mechanical characterisation of the chromium nitride hard coating deposited on the silicon and glass substrate', *Int. J. Autom. Mech. Eng.*, 2017, **14**, (1), pp. 3872–3886
[13] Liu C., Bi Q., Leyland A., *ET AL.*: 'An electrochemical impedance spectroscopy study of the corrosion behaviour of PVD coated steels in 0.5 N NaCl aqueous solution: part II. EIS interpretation of corrosion behaviour', *Corros. Sci.,* 2003, **45**, pp. 1257–1273
[14] Zalnezhad E., Sarhan A.A.D.M., Hamdi M.: 'Surface hardness prediction of CrN thin film coating on Al7075-T6 alloy using fuzzy logic system', *Int. J. Precis. Eng. Manuf.*, 2013, **14**, (3), pp. 467–473
[15] Bouzida K., Beliardouh N.E., Nouveau C.: 'Wear and corrosion resistance of CrN-based coatings deposited by R.F magnetron sputtering', *Tribol. Ind.*, 2015, **37**, (1), pp. 60–65
[16] Kennedy D.M., Xue Y., Mihaylova E.: 'Current and future applications of surface engineering', *Eng. J. Tech.*, 2005, **59**, pp. 287–292
[17] Sánchez G., Abdallah B., Tristant P., *ET AL.*: 'Microstructure and mechanical properties of ALN films obtained by plasma enhanced chemical vapor deposition', *J. Mater. Sci.*, 2009, **44**, (22), pp. 6125–6134
[18] Perillo P.M.: 'Properties of CrN coating prepared by physical vapour deposition', *Am. J. Mater. Sci. Appl.*, 2015, **3**, (2), pp. 38–43
[19] Subramanian B., Jayachandran M.: 'Preparation of chromium oxynitride and chromium nitride films by DC reactive magnetron sputtering and their material properties', *Corros. Eng. Sci. Technol.*, 2013, **46**, (4), pp. 554–561
[20] Montesano L., Gelfi M., Pola A., *ET AL.*: 'Corrosion resistance of CrN PVD coatings: comparison among different deposition techniques', *Metall. Ital.*, 2013, (2), pp. 3–11
[21] Jazmati A.K., Abdallah B.: 'Optical and structural study of ZnO thin films deposited by RF magnetron sputtering at different thicknesses: a comparison with single crystal', *Mater. Res.*, 2018, **21**, pp. 1–6
[22] Merie V.V., Negrea G., Modi E.: 'The influence of substrate temperature on the tribo-mechanical properties of chromium nitride thin films', *IOP Conf. Ser., Mater. Sci. Eng.*, 2016, **147**, p. 012020
[23] Abdallah B., Jazmati A.K., Kakhia M.: 'Physical, optical and sensing properties of sprayed zinc doped tin oxide films', *Optik*, 2018, **158**, pp. 1113–1122
[24] Abdallah B., Kakhia M., Alssadat W., *ET AL.*: 'Deposition of $Ti6Al_4V$ thin films by DC magnetron sputtering: effect of the current on structural, corrosion and mechanical properties', *Iran. J. Sci. Technol.*, 2019, **43**, pp. 1957–1965
[25] Shah H.N., Chawla V., Jayaganthan R., *ET AL.*: 'Microstructural characterizations and hardness evaluation of D.C. reactive magnetron sputtered CrN thin films on stainless steel substrate', *Bull. Mater. Sci.*, 2010, **33**, (2), pp. 103–110
[26] Abdallah B., Jazmati A.K., Refaai R.: 'Oxygen effect on structural and optical properties of ZnO thin films deposited by RF magnetron sputtering', *Mater. Res.*, 2017, **20**, (3), pp. 607–612
[27] Shah H.N., Jayaganthan R., Kaur D.: 'Effect of sputtering pressure and temperature on DC magnetron sputtered CrN films', *Surf. Eng.*, 2010, **26**, pp. 629–637
[28] Rahmane S., Djouadi M.A., Aida M.S., *ET AL.*: 'Power and pressure effects upon magnetron sputtered aluminum doped ZnO films properties', *Thin Solid Films*, 2010, **519**, (1), pp. 5–10
[29] Chawla V., Jayaganthan R., Chandra R.: 'Structural characterizations of magnetron sputtered nanocrystalline TiN thin films', *Mater. Charact.*, 2008, **59**, pp. 1015–1020
[30] Abdallah B., Jazmat A.K., Nounou F.: 'Morphological and structural characterization of ZnO nanostructure films deposited on plasma etched silicon substrates', *J. Nanostruct.*, 2018, **10**, pp. 185–197
[31] Abdallah B., Duquenne C., Besland M.P., *ET AL.*: 'Thickness and substrate effects on AlN thin film growth at room temperature', *Eur. Phys. J., Appl. Phys.*, 2008, **43**, (3), pp. 309–313
[32] Song G.-H., Yang X.-P., Xiong G.-L., *ET AL.*: 'The corrosive behavior of Cr/CrN multilayer coatings with different modulation periods', *Vacuum*, 2013, **89**, pp. 136–141
[33] Frankel G.S.: 'Fundamentals of corrosion kinetics', in Hughes A.E., Mol J.M.C., Zheludkevich M.L., *ET AL.* (Eds.): 'Active protective coatings: new-generation coatings for metals' (Springer, Netherlands, 2016), pp. 17–32
[34] Wang Z.B., Lu J., Lu K.: 'Wear and corrosion properties of a low carbon steel processed by means of SMAT followed by lower temperature chromizing treatment', *Surf. Coat. Technol.*, 2006, **201**, (6), pp. 2796–2801
[35] Zykova A., Safonov V., Walkowich J., *ET AL.*: 'Corrosion properties of nitride, oxide and multilayer coatings on stainless steel and titanium-based substrates', *J. Phys., Conf. Ser.*, 2010, **223**, (1), p. 012024
[36] Braic M., Zamfira S., Balaceanu M., *ET AL.*: 'Corrosion resistance of tin coated 316l stainless steel in artificial physiological solution', *J. Optoelectron. Adv. Mater.*, 2003, **5**, (2), pp. 503–510